Int. J. Solids Structures Vol. 22, No. 11, pp. 1259–1277, 1986
Printed in Great Britain.

0020–7683/86 $3.00 + .00
Pergamon Journals Ltd.

STRENGTH OF COMPOSITE MATERIALS WITH SMALL CRACKS IN THE MATRIX

HENRIK STANG
Department of Structural Engineering, Technical University of Denmark,
Building 118, DK-2800 Lyngby, Denmark

(*Received* 30 *May* 1985; *in revised form* 20 *November* 1985)

Abstract—Often composite materials are designed primarily with the aim of improving the strength of the matrix material rather than achieving improvement of the stiffness. This is usually the case when the matrix is a low strength brittle type material. The strength of such a matrix material is usually governed by the initial flaws present in the material. These flaws or cracks can either be large or small compared to the microstructure of the composite material. In this paper "small" flaws are considered. Both the small flaws and the reinforcing particles are modelled by ellipsoidal inclusions and included in a composite material theory which is able to give an account of the interaction between the inclusions. In order to describe the strengthening effect of the reinforcing inclusions, the energy release rate for a representative penny-shaped matrix crack in the composite material is determined and compared to the energy release rate of the same crack present in the otherwise homogeneous matrix material.

1. INTRODUCTION

Analytical determination of the strength of composite materials is in general a very difficult matter due to the large variety of different failure modes in a composite material. In a review article Dharan[1] identifies ten different failure modes for a fibre reinforced material and it is of course impossible to describe all these failure modes within the framework of one analytical model.

However, the failure process of a given class of composite materials is often dominated by a few failure modes. The composite materials with a brittle matrix and one, two, or more types of tough inclusions constitute such a class. The typical failure modes in this type of materials are matrix cracking and debonding of the interface between matrix and inclusions. This paper deals with matrix cracking in a composite material containing inclusions of arbitrary, ellipsoidal shape. It is assumed that the matrix cracks are "small", i.e. small compared to the microstructure of the composite material. This means that the matrix cracks (or microcracks) and the reinforcing inclusions can be considered as independent inclusion types imbedded in the matrix and interacting over a certain distance.

When the matrix cracks are large in a fibre reinforced material, then an entirely different situation arises because of the crack bridging fibres and the ensuing direct interaction between the fibres and the crack. Large microcracks have been treated by, e.g. Korczynskyj *et al.*[2], Selvadurai[3], Mori and Mura[4], and Stang[5]. The general procedure is that the matrix crack is modelled by a penny-shaped crack. The crack closing forces exerted by the fibres on the matrix are related to the crack opening and localized either on the crack surface[3, 4] or at some distance from the crack surface[2, 5]. The strengthening effect is finally evaluated by means of energy considerations as in Refs [2, 5] or by the determination of modified stress intensity factors as in Refs [3, 4].

The effect and growth of small microcracks are usually evaluated by means of a composite material theory. Homogeneous materials containing *only* microcracks have been described by means of a composite material theory in a number of papers in the past. The elastic moduli of materials containing penny-shaped microcracks under dilute conditions have been determined by Bristow[6] and Walsh[7] in the randomized isotropic case and by Salganik[8] in the isotropic and the aligned, transversely isotropic case.

Larger crack concentrations have been treated by Budiansky and O'Connell[9]. In order to account for the interaction between the cracks, the self-consistent scheme was adopted. Budiansky and O'Connell considered randomly distributed cracks which allowed the self-consistent technique to be used in the way it was originally stated by Budiansky[10]

and Hill[11]. The case of non-randomly distributed cracks under non-dilute conditions have been treated by Hoenig[12] again using the self-consistent technique. A general description of the self-consistent technique for anisotropic composites has been given by Willis[13].

Budiansky and O'Connell's results have been generalized by Horii and Nemat-Nasser[14] who considered the situation where some of the cracks close or undergo frictional sliding. Also Horii and Nemat-Nasser adopted the self-consistent scheme and the results of Budiansky and O'Connell are derived once more as a special case.

Levin[15] followed a different approach in order to determine the elastic moduli for a body with microcracks. Levin develops in Ref. [15] a composite material theory which takes account of the interaction between the not necessarily randomized inclusions. However, Levin still uses Eshelby's solution[16] for one ellipsoidal inclusion in an infinite isotropic matrix. With this theory the elastic moduli for a body with randomized or non-randomized microcracks can be determined with a simple limiting process. The results of Salganik[8] are re-established in the special case of dilute conditions.

With a general composite material theory it is a relatively straightforward matter to describe a *composite material* containing microcracks. The composite material theory in question must be able to describe composite materials with two or more inclusion types (reinforcing inclusions and cracks) under non-dilute conditions. Clearly the self-consistent theory can be used for this purpose. Laws *et al.*[17] used the self-consistent theory to describe a fibre reinforced material containing microcracks in the matrix. Taya[18] has described a similar material by means of a composite material theory for a material containing two kinds of ellipsoidal inclusions developed by Taya and Chou[19]. The basis of this analysis is the so-called back stress analysis introduced by Mori and Tanaka[20]. Taya determines the stiffness changes caused by matrix crack systems in a short fibre composite material and also the energy release rate for a representative penny-shaped matrix crack in the composite material.

Levin's composite material theory[15] is also applicable to the description of composite materials with microcracks. However, Levin's theory has to be generalized in order to deal with more than one inclusion type. This will be done in the following sections and it will be shown that the strengthening effect of the reinforcing inclusions can be described by one fourth order tensor without assuming anything about the length and orientation of the reinforcing ellipsoidal inclusions.

2. BASIC RELATIONS

The composite materials considered here are materials of the matrix/inclusion type. The matrix and the inclusions are assumed to be isotropic and linear elastic.

Let a Cartesian coordinate system (x_1, x_2, x_3) be given and consider a representative volume element (RVE) (representative in the sense explained by Hill[21]) of the composite material in question. The volume element has a volume V with a surface $\delta(V)$. In this RVE macroscopically homogeneous stress and strain fields are prescribed by the boundary conditions:

$$\sigma_{ij} n_j = \sigma^*_{ij} n_j \qquad \text{on } \delta(V) \tag{1}$$

or

$$u_i = \varepsilon^*_{ij} x_j \qquad \text{on } \delta(V) \tag{2}$$

where σ_{ij} denotes the stress tensor, u_i the displacements, n_i the outward unit normal to $\delta(V)$, and σ^*_{ij} and ε^*_{ij} are symmetric tensors, constant in space.

It is a well-known fact (see Ref. [21]) that the volume averages of stress and strain in the RVE are given by

$$\{\boldsymbol{\sigma}\}^V = \frac{1}{V} \int_V \boldsymbol{\sigma} \, \mathrm{d}V = \boldsymbol{\sigma}^* \tag{3}$$

when the boundary condition, eqn (1) is given, and by

$$\{\varepsilon\}^V = \frac{1}{V}\int_V \varepsilon \, dV = \varepsilon^* \tag{4}$$

when eqn (2) is given. (Following Hill we write σ and ε as shorthand for the stress and strain tensors σ_{ij} and ε_{ij}.)

Given the boundary conditions, eqn (1) or (2), the stiffness and compliance of the composite material are defined by

$$\{\sigma\}^V = \mathbf{L}^C\{\varepsilon\}^V \tag{5}$$

and

$$\{\varepsilon\}^V = \mathbf{M}^C\{\sigma\}^V. \tag{6}$$

$\mathbf{L}^C$ and $\mathbf{M}^C$ are shorthand for L^C_{ijkl} and M^C_{ijkl} and the product on the right-hand side of eqns (5) and (6) involves summation over the two index pairs: $L^C_{ijkl}\{\varepsilon\}^V_{kl}$ and $M^C_{ijkl}\{\sigma\}^V_{kl}$.

The matrix phase of the composite material is designated phase 0 while the inclusion phases are designated phase $1, 2, \ldots, n$. Thus, the composite material contains $n+1$ phases.

The physical quantities characterizing phase i are all denoted with superscript "i" ($i = 0, 1, \ldots, n$). Now, in order to be able to distinguish between powers and labels identifying the phase in question, *powers are always separated from the base with a parenthesis*, thus, e.g. a^3 means the physical quantity "a" characterizing phase 3 while $(a)^3$ denotes "a" raised to the third power. The use of subscripts is restricted to the indication of tensor component only.

Introducing the relations between the volume average of the stress/strain fields in the RVE and the volume average of the stress/strain fields in each phase (see Ref. [21]):

$$\{\sigma\}^{V^i} = \frac{1}{V^i}\int_{V^i} \sigma \, dV = \mathbf{B}^i\{\sigma\}^V \qquad i = 0, \ldots, n \tag{7}$$

$$\{\varepsilon\}^{V^i} = \frac{1}{V^i}\int_{V^i} \varepsilon \, dV = \mathbf{A}^i\{\varepsilon\}^V \qquad i = 0, \ldots, n \tag{8}$$

and introducing the volume concentrations $c^0, c^1, \ldots, c^n$, then $\mathbf{L}^C$ and $\mathbf{M}^C$ can be written as

$$\mathbf{L}^C = \mathbf{L}^0 + \sum_{i=1}^{n} c^i(\mathbf{L}^i - \mathbf{L}^0)\mathbf{A}^i \tag{9}$$

$$\mathbf{M}^C = \mathbf{M}^0 + \sum_{i=1}^{n} c^i(\mathbf{M}^i - \mathbf{M}^0)\mathbf{B}^i. \tag{10}$$

Given the boundary conditions, eqns (1) and (2), Levin shows (see Refs [15, 22]) that the stress and strain fields in the RVE are given by

$$\sigma(\mathbf{x}) = \sigma^* + \int_V \Gamma(\mathbf{x}, \zeta)[\delta\mathbf{M}(\zeta)\sigma(\zeta) - \{\delta\mathbf{M}\cdot\sigma\}^V] \, dV(\zeta) \tag{11}$$

and

$$\varepsilon(\mathbf{x}) = \varepsilon^* - \int_V \mathbf{G}(\mathbf{x}, \zeta)[\delta\mathbf{L}(\zeta)\varepsilon(\zeta) - \{\delta\mathbf{L}\varepsilon\}^V] \, dV(\zeta) \tag{12}$$

with

$$G(\mathbf{x}, \zeta)_{ijkl} = \frac{1}{2}\left(\frac{\partial^2 g(\mathbf{x}, \zeta)_{im}}{\partial x_j \, \partial \zeta_n} + \frac{\partial^2 g(\mathbf{x}, \zeta)_{jm}}{\partial x_i \, \partial \zeta_n}\right) I_{mnkl} \tag{13}$$

and

$$\Gamma(\mathbf{x},\zeta) = \mathbf{L}^0\mathbf{G}(\mathbf{x},\zeta)\mathbf{L}^0 - \delta(\mathbf{x}-\zeta)\mathbf{L}^0. \tag{14}$$

Here $\delta(\mathbf{x}-\zeta)$ is the 3D-Dirac's delta function with

$$\int_V \delta(\mathbf{x}-\zeta)\,\mathrm{d}V(\zeta) = \begin{cases} 1 & \text{for } x \in V \\ 0 & \text{for } x \notin V. \end{cases} \tag{15}$$

The two point function $g(\mathbf{x},\zeta)_{ij}$ is a Green's function for the homogeneous RVE with stiffness $\mathbf{L}^0$ giving the displacements from a single force P_i in V

$$u(\mathbf{x})_i = g(\mathbf{x},\zeta)_{ij}P(\zeta)_j \qquad \mathbf{x},\zeta \in V. \tag{16}$$

It is assumed that

$$\mathbf{g}(\mathbf{x},\zeta) \equiv \mathbf{0} \qquad \mathbf{x} \in \delta(V),\ \zeta \in V. \tag{17}$$

The fourth order tensor $\mathbf{I}$ is the identity fourth order tensor given by

$$I_{ijkl} = \tfrac{1}{2}(\delta_{ik}\delta_{jl} + \delta_{il}\delta_{jk}) \tag{18}$$

where δ_{ij} is Kronecker's delta. The tensor $\mathbf{I}$ is included in eqn (13) in order to make the last index pair symmetric. The tensors $\delta\mathbf{L}$ and $\delta\mathbf{M}$ represent the variations in stiffness and compliance with respect to the matrix, i.e.

$$\delta\mathbf{L}(\mathbf{x}) = \mathbf{L}^i - \mathbf{L}^0 \qquad \text{when} \quad \mathbf{x} \in V^i \quad i = 0, 1, \ldots, n \tag{19}$$

and

$$\delta\mathbf{M}(\mathbf{x}) = \mathbf{M}^i - \mathbf{M}^0 \qquad \text{when} \quad \mathbf{x} \in V^i \quad i = 0, 1, \ldots, n. \tag{20}$$

Introducing the Green's function for an infinite, isotropic, homogeneous space with stiffness $\mathbf{L}^0, \mathbf{g}^\infty$, instead of $\mathbf{g}$, then eqns (11) and (12) can be written as

$$\boldsymbol{\sigma} = \boldsymbol{\sigma}^* + \int_V \Gamma^\infty[\delta\mathbf{M}\boldsymbol{\sigma} - \{\delta\mathbf{M}\boldsymbol{\sigma}\}^V]\,\mathrm{d}V \tag{21}$$

and

$$\boldsymbol{\varepsilon} = \boldsymbol{\varepsilon}^* + \int_V \mathbf{G}^\infty[\delta\mathbf{L}\boldsymbol{\varepsilon} - \{\delta\mathbf{L}\boldsymbol{\varepsilon}\}^V]\,\mathrm{d}V \tag{22}$$

with

$$G^\infty_{ijkl} = \frac{1}{2}\left(\frac{\partial^2 g^\infty_{im}}{\partial x_j\,\partial x_n} + \frac{\partial^2 g^\infty_{jm}}{\partial x_i\,\partial x_n}\right) I_{mnkl} \tag{23}$$

and

$$\Gamma^\infty = -(\mathbf{L}^0\mathbf{G}^\infty\mathbf{L}^0 + \mathbf{L}^0\delta) \tag{24}$$

where δ is shorthand for the 3D-Dirac function.

The volume of one ellipsoidal inclusion belonging to phase i is now designated ι^i and all inclusions belonging to phase i are assumed to have the same size and volume but not necessarily the same orientation in space. A point of observation $\mathbf{x}^i$ is fixed in an inclusion ι^i

and it is assumed that (see Ref. [15])

$$\int_{V\setminus v^i} \mathbf{G}^{\infty}(\mathbf{x}^i,\zeta)\delta\mathbf{L}(\zeta)\boldsymbol{\varepsilon}(\zeta)\,\mathrm{d}V(\zeta) \cong \int_{V\setminus v^i} \mathbf{G}^{\infty}(\mathbf{x}^i,\zeta)\{\delta\mathbf{L}\boldsymbol{\varepsilon}\}^{V}\,\mathrm{d}V(\zeta) \tag{25}$$

and

$$\int_{V\setminus v^i} \boldsymbol{\Gamma}^{\infty}(\mathbf{x}^i,\zeta)\delta\mathbf{M}(\zeta)\boldsymbol{\sigma}(\zeta)\,\mathrm{d}V(\zeta) \cong \int_{V\setminus v^i} \boldsymbol{\Gamma}^{\infty}(\mathbf{x}^i,\zeta)\{\delta\mathbf{M}\boldsymbol{\sigma}\}^{V}\,\mathrm{d}V(\zeta). \tag{26}$$

Thus, it is assumed that the influence of one inclusion from the rest of the inclusions can be equivalated with the influence from stress and strain fields which are constant in space and equivalent to the volume average of the perturbation fields.

Now the average stress and strain field in v^i can be calculated as

$$\{\boldsymbol{\sigma}\}^{v^i} = \boldsymbol{\sigma}^{*} - \mathbf{Q}^i(\{\delta\mathbf{M}\boldsymbol{\sigma}\}^{v^i} - \{\delta\mathbf{M}\boldsymbol{\sigma}\}^{V}) \tag{27}$$

$$\{\boldsymbol{\varepsilon}\}^{v^i} = \boldsymbol{\varepsilon}^{*} - \mathbf{P}^i(\{\delta\mathbf{L}\boldsymbol{\varepsilon}\}^{v^i} - \{\delta\mathbf{L}\boldsymbol{\varepsilon}\}^{V}) \tag{28}$$

given the boundary conditions, eqns (1) and (2), and the relations

$$\mathbf{Q}^i(\mathbf{x}^i) = -\int_{v^i} \boldsymbol{\Gamma}^{\infty}(\mathbf{x}^i,\zeta)\,\mathrm{d}V(\zeta) \tag{29}$$

and

$$\mathbf{P}^i(\mathbf{x}^i) = -\int_{v^i} \mathbf{G}^{\infty}(\mathbf{x}^i,\zeta)\,\mathrm{d}V(\zeta). \tag{30}$$

The tensors $\mathbf{Q}^i$ and $\mathbf{P}^i$ are homogeneous in v^i and related by

$$\mathbf{Q}^i = \mathbf{L}^0 - \mathbf{L}^0\mathbf{P}^i\mathbf{L}^0. \tag{31}$$

The P- and Q-tensors are furthermore related to Eshelby's S-tensor (see Ref. [16]) by the relation

$$\mathbf{P}^i = \mathbf{S}^i\mathbf{M}^0 \tag{32}$$

where $\mathbf{S}^i$ is the S-tensor related to phase i.

Since the inclusions in phase i all have the same size and shape, the average stress field in a specific inclusion v^i only depends on the orientation of the inclusion. Denoting by $\{\{\boldsymbol{\sigma}\}^{v^i}\}^{\omega}$ the average of the (average) stress fields taken over all the orientations which represents inclusions in phase i, then

$$\{\boldsymbol{\sigma}\}^{V^i} = \{\{\boldsymbol{\sigma}\}^{v^i}\}^{\omega} \tag{33}$$

and since

$$\{\delta\mathbf{M}\boldsymbol{\sigma}\}^{V} = \sum_{j=1}^{n} c^j(\mathbf{M}^j - \mathbf{M}^0)\{\{\boldsymbol{\sigma}\}^{v^j}\}^{\omega} \tag{34}$$

and

$$\{\delta\mathbf{L}\boldsymbol{\varepsilon}\}^{V} = \sum_{j=1}^{n} c^j(\mathbf{L}^j - \mathbf{L}^0)\{\{\boldsymbol{\varepsilon}\}^{v^j}\}^{\omega} \tag{35}$$

the following systems of equations can be derived from eqns (27) and (28)

$$\begin{bmatrix} \mathbf{R}^{11} & -\mathbf{R}^{12} & -\mathbf{R}^{13} & \dots & -\mathbf{R}^{1n} \\ -\mathbf{R}^{21} & \mathbf{R}^{22} & -\mathbf{R}^{23} & \dots & -\mathbf{R}^{2n} \\ \dots & \dots & \dots & \dots & \dots \\ -\mathbf{R}^{n1} & -\mathbf{R}^{n2} & -\mathbf{R}^{n3} & \dots & \mathbf{R}^{nn} \end{bmatrix} \begin{bmatrix} \{\boldsymbol{\sigma}\}^{V^1} \\ \{\boldsymbol{\sigma}\}^{V^2} \\ \vdots \\ \{\boldsymbol{\sigma}\}^{V^n} \end{bmatrix} = \begin{bmatrix} \{\mathbf{T}^1\}^{\omega} \\ \{\mathbf{T}^2\}^{\omega} \\ \vdots \\ \{\mathbf{T}^n\}^{\omega} \end{bmatrix} \boldsymbol{\sigma}^* \tag{36a}$$

where

$$\mathbf{R}^{ii} = \mathbf{I} - c^i \{\mathbf{T}^i \mathbf{Q}^i\}^{\omega} (\mathbf{M}^i - \mathbf{M}^0) \qquad \text{(no summation)} \tag{36b}$$

$$\mathbf{R}^{ij} = \{\mathbf{T}^i \mathbf{Q}^i\}^{\omega} (\mathbf{M}^j - \mathbf{M}^0) c^j \qquad \text{(no summation and } i \neq j\text{)} \tag{36c}$$

$$\mathbf{T}^i = (\mathbf{I} + \mathbf{Q}^i (\mathbf{M}^i - \mathbf{M}^0))^{-1} \qquad \text{(no summation).} \tag{36d}$$

And

$$\begin{bmatrix} \mathbf{N}^{11} & -\mathbf{N}^{12} & -\mathbf{N}^{13} & \dots & -\mathbf{N}^{1n} \\ -\mathbf{N}^{21} & \mathbf{N}^{22} & -\mathbf{N}^{23} & \dots & -\mathbf{N}^{2n} \\ \dots & \dots & \dots & \dots & \dots \\ -\mathbf{N}^{n1} & -\mathbf{N}^{n2} & -\mathbf{N}^{n3} & \dots & \mathbf{N}^{nn} \end{bmatrix} \begin{bmatrix} \{\boldsymbol{\varepsilon}\}^{V^1} \\ \{\boldsymbol{\varepsilon}\}^{V^2} \\ \vdots \\ \{\boldsymbol{\varepsilon}\}^{V^n} \end{bmatrix} = \begin{bmatrix} \{\mathbf{H}^1\}^{\omega} \\ \{\mathbf{H}^2\}^{\omega} \\ \vdots \\ \{\mathbf{H}^n\}^{\omega} \end{bmatrix} \boldsymbol{\varepsilon}^* \tag{37a}$$

where

$$\mathbf{N}^{ii} = \mathbf{I} - c^i \{\mathbf{H}^i \mathbf{P}^i\}^{\omega} (\mathbf{L}^i - \mathbf{L}^0) \qquad \text{(no summation)} \tag{37b}$$

$$\mathbf{N}^{ij} = \{\mathbf{H}^i \mathbf{P}^i\}^{\omega} (\mathbf{L}^j - \mathbf{L}^0) c^j \qquad \text{(no summation and } i \neq j\text{)} \tag{37c}$$

$$\mathbf{H}^i = (\mathbf{I} + \mathbf{P}^i (\mathbf{L}^i - \mathbf{L}^0))^{-1} \qquad \text{(no summation).} \tag{37d}$$

In all the equations (36b)–(36d) and (37b)–(37d) we have $i, j \in \{1, 2, \dots, n\}$.

The solutions of eqns (36a)–(36d) and (37a)–(37d) give the $\mathbf{B}^i$ and $\mathbf{A}^i$ tensors, and $\mathbf{L}^0$ and $\mathbf{M}^0$ can now be determined by eqns (9) and (10).

In a number of special cases the systems of equations are reduced considerably. Furthermore, it should be noted that the systems (36a)–(36d) and (37a)–(37d) are completely equivalent: the system (37a)–(37d) results from (36a)–(36d) by substituting $\mathbf{L}^i$ for $\mathbf{M}^i$ and $\mathbf{P}^i$ for $\mathbf{Q}^i$. Thus, it is only necessary to write down the systems of equations which determine, e.g. the B^i-tensors.

3. SPECIAL CASES

We assume that the composite material in question consists of three phases: a matrix and two inclusion types. If inclusion type 1 is aligned and the other (type 2) is non-aligned, possibly randomized, then it can be shown that eqns (36a)–(36d) reduces to

$$\begin{bmatrix} \mathbf{R}^{11} & -\mathbf{R}^{12} \\ -\mathbf{R}^{21} & \mathbf{R}^{22} \end{bmatrix} \begin{bmatrix} \{\boldsymbol{\sigma}\}^{V^1} \\ \{\boldsymbol{\sigma}\}^{V^2} \end{bmatrix} = \begin{bmatrix} \boldsymbol{\sigma}^* \\ \boldsymbol{\sigma}^* \end{bmatrix} \tag{38a}$$

with

$$\mathbf{R}^{11} = \mathbf{I} + (1 - c^1) \mathbf{Q}^1 (\mathbf{M}^1 - \mathbf{M}^0) \tag{38b}$$

$$\mathbf{R}^{12} = \mathbf{Q}^1 (\mathbf{M}^2 - \mathbf{M}^0) c^2 \tag{38c}$$

$$\mathbf{R}^{21} = (\{\mathbf{T}^2\}^{\omega})^{-1}\{\mathbf{T}^2\mathbf{Q}^2\}^{\omega}(\mathbf{M}^1 - \mathbf{M}^0)c^1 \tag{38d}$$

$$\mathbf{R}^{22} = (\{\mathbf{T}^2\}^{\omega})^{-1}\{\mathbf{I} - c^2\{\mathbf{T}^2\mathbf{Q}^2\}^{\omega}(\mathbf{M}^2 - \mathbf{M}^0)\} \tag{38e}$$

where

$$\mathbf{T}^2 = (\mathbf{I} + \mathbf{Q}^2(\mathbf{M}^2 - \mathbf{M}^0))^{-1}. \tag{38f}$$

Solving eqns (38a)–(38f) and introducing eqns (7) and (10) we get the following expression for $\mathbf{M}^C$:

$$\begin{aligned}\mathbf{M}^C = \mathbf{M}^0 &+ c^1(\mathbf{M}^1 - \mathbf{M}^0)\{\mathbf{R}^{11} - \mathbf{R}^{12}(\mathbf{R}^{22} + \mathbf{R}^{12})^{-1}(\mathbf{R}^{11} + \mathbf{R}^{21})\}^{-1} \\ &+ c^2(\mathbf{M}^2 - \mathbf{M}^0)\{\mathbf{R}^{22} - \mathbf{R}^{21}(\mathbf{R}^{11} + \mathbf{R}^{21})^{-1}(\mathbf{R}^{22} + \mathbf{R}^{12})\}^{-1}.\end{aligned} \tag{39}$$

In the special case of two aligned inclusion phases (the two phases need not be aligned in the same direction) the above expressions for $\mathbf{R}^{21}$ and $\mathbf{R}^{22}$ are simply replaced by

$$\mathbf{R}^{21} = \mathbf{Q}^2(\mathbf{M}^1 - \mathbf{M}^0)c^1 \tag{40a}$$

$$\mathbf{R}^{22} = \mathbf{I} + (1 - c^2)\mathbf{Q}^2(\mathbf{M}^2 - \mathbf{M}^0). \tag{40b}$$

The special cases of one aligned and one non-aligned inclusion phase can easily be derived from eqns (38a)–(38f). It is interesting to note that when one aligned inclusion phase is present under dilute conditions, then the well-known relation

$$\mathbf{M}^C = \mathbf{M}^0 + c^1(\mathbf{M}^1 - \mathbf{M}^0)[\mathbf{I} + \mathbf{Q}^1(\mathbf{M}^1 - \mathbf{M}^0)]^{-1} \tag{41}$$

or equivalently

$$\mathbf{L}^C = \mathbf{L}^0 + c^1(\mathbf{L}^1 - \mathbf{L}^0)[\mathbf{I} + \mathbf{P}^1(\mathbf{L}^1 - \mathbf{L}^0)]^{-1} \tag{42}$$

is re-established.

4. INTRODUCTION OF MICROCRACKS

Microcracks in the matrix material are modelled by penny-shaped cracks, i.e. by flat axially symmetrical ellipsoids. Consider an axially symmetrical ellipsoidal inclusion. The surface of the inclusion will be described by the following equation:

$$\left(\frac{x_1}{a}\right)^2 + \left(\frac{x_2}{a}\right)^2 + \left(\frac{x_3}{c}\right)^2 = 1. \tag{43}$$

The aspect ratio of the inclusions is defined as

$$l = \frac{c}{a}. \tag{44}$$

When the microcrack phase of the composite material is designated as phase 1, then the limit

$$l^1 \to 0 \qquad \text{with} \quad \mathbf{L}^1 = \mathbf{0}$$

represents the modelling of the microcracks (l^1 defines the aspect ratio and $\mathbf{L}^1$ represents the stiffness of phase 1).

In order to investigate this limiting process the simple case of aligned cracks under dilute conditions (or simply one penny-shaped crack in an infinite medium) is considered.

The case is described by eqn (42). Introducing $\mathbf{L}^1 = \mathbf{0}$, eqn (42) can be written as

$$\mathbf{L}^C = \mathbf{L}^0[\mathbf{I} - c^1(\mathbf{I} - \mathbf{S}^1)^{-1}]. \tag{45}$$

The equivalent eqn (41) can be rewritten as

$$\mathbf{M}^C = \mathbf{M}^0 + c^1[\mathbf{M}^0(\mathbf{M}^1 - \mathbf{M}^0)^{-1} + \mathbf{I} - \mathbf{S}^1]^{-1}\mathbf{M}^0 = [\mathbf{I} + c^1(\mathbf{I} - \mathbf{S}^1)^{-1}]\mathbf{M}^0 \tag{46}$$

since $\mathbf{M}^0(\mathbf{M}^1 - \mathbf{M}^0)^{-1} = \mathbf{M}^0\mathbf{L}^1(\mathbf{I} - \mathbf{M}^0\mathbf{L}^1)^{-1} = \mathbf{0}$, when $\mathbf{L}^1 = \mathbf{0}$. However, the tensor $(\mathbf{I} - \mathbf{S}^1)^{-1}$ becomes singular (i.e. the inverse does not exist) when $l^1 \to 0$, while $c^1 \to 0$. Thus c^1 is rewritten as

$$c^1 = \beta^1 l^1 \tag{47}$$

with

$$\beta^1 = \frac{4\pi}{3}\frac{n(a)^3}{V}. \tag{48}$$

The parameter β is usually denoted "the crack density parameter" and n designates the total number of penny-shaped cracks in V.

The tensor $l^1(\mathbf{I} - \mathbf{S}^1)^{-1}$ has a finite value for $l^1 \to 0$, and we can define a new tensor, the F-tensor, as the limit

$$\mathbf{F}^1 = \lim_{l^1 \to 0} (l^1(\mathbf{I} - \mathbf{S}^1)^{-1}). \tag{49}$$

Since the inclusions under consideration are axially symmetrical, the corresponding S-tensor is transversely isotropic. And since the I-tensor is isotropic (because δ_{ij} is isotropic, see eqn (18)) it follows from eqn (49) that the F-tensor is transversely isotropic.

The F-tensor can easily be determined when using the decomposition technique for transversely isotropic fourth order tensors described by Walpole[23]. First the S-tensor is decomposed in the way described in Ref. [23]. (The decomposed form of the S-tensor is given in Ref. [5].) Linearizing the S-tensor as a function of l^1 for $l^1 \sim 0$, we get

$$\mathbf{S}^1(l^1) = \mathbf{S}^1(0) + l^1\mathbf{\Sigma}^1 \tag{50}$$

with

$$\mathbf{S}^1(0) = \left(0, 1, 0, 1, \frac{\nu^0}{1-\nu^0}, 0\right) \tag{51}$$

and

$$\mathbf{\Sigma}^1 = \Big(6, -4(1-2\nu^0), (7-8\nu^0), -4(2-\nu^0), -2(1+4\nu^0), -2(1-2\nu^0)\Big)\frac{\pi}{16(1-\nu^0)} \tag{52}$$

where ν^0 is Poisson's ratio for the matrix.

Now it is easy to show that

$$\mathbf{F}^1 = \left(0, \frac{(1-\nu^0)^2}{(1-2\nu^0)}, 0, \frac{(1-\nu^0)}{(2-\nu^0)}, \frac{(1-\nu^0)\nu^0}{(1-2\nu^0)}, 0\right)\frac{4}{\pi} \tag{53}$$

remembering that

$$\mathbf{I} = (1,1,1,1,0,0) \tag{54}$$

and using the formulas for inversion of transversely isotropic tensors given in Ref. [23].

Thus the stiffness and compliance of a homogeneous material with aligned microcracks under dilute conditions can be written as

$$\mathbf{L}^C = \mathbf{L}^0(\mathbf{I} - \beta^1\mathbf{F}^1) \tag{55}$$

and

$$\mathbf{M}^C = (\mathbf{I} + \beta^1\mathbf{F}^1)\mathbf{M}^0 \tag{56}$$

according to eqns (45) and (46).

A similar limiting process can be made when we are dealing with non-dilute conditions and cracks in a composite material rather than cracks in a homogeneous material. Equations (38a)–(38f) and (39) form the basis of such an analysis. Phase 1 is again representing the cracks or one representative crack, while phase 2 represents the reinforcing inclusions. Note that no assumptions are made about the orientation and shape of the phase 2 inclusions.

Writing eqn (39) as

$$\mathbf{M}^C = \mathbf{M}^C(\mathbf{M}^0, c^1, l^1, \mathbf{L}^1, c^2, l^2, \mathbf{L}^2) \tag{57}$$

it is possible to show that

$$\lim_{l^1 \to 0} \mathbf{M}^C(\mathbf{M}^0, \beta^1 l^1, l^1, \mathbf{0}, c^2, l^2, \mathbf{L}^2) = [\mathbf{I} + c^2(\mathbf{R}^2)^{-1} + \beta^1\mathbf{U}^2\mathbf{F}^1]\mathbf{M}^0. \tag{58}$$

The derivation is somewhat tedious but it represents no special difficulties once eqn (49) is established.

The R-tensor in eqn (58) is given by

$$\mathbf{R}^2 = (\{(\mathbf{M} + \mathbf{I} - \mathbf{S}^2)^{-1}\}^\omega)^{-1}[\mathbf{I} - c^2\{(\mathbf{M} + \mathbf{I} - \mathbf{S}^2)^{-1}(\mathbf{I} - \mathbf{S}^2)\}^\omega] \tag{59}$$

with

$$\mathbf{M} = \mathbf{M}^0(\mathbf{M}^2 - \mathbf{M}^0)^{-1} \tag{60}$$

while the U-tensor is given by

$$\mathbf{U}^2 = \mathbf{I} + c^2((\{(\mathbf{M} + \mathbf{I} - \mathbf{S}^2)^{-1}(\mathbf{I} - \mathbf{S}^2)\}^\omega)^{-1} - c^2\mathbf{I})^{-1}. \tag{61}$$

In the special case where phase 2 consists of aligned inclusions, the expression for U^2 is simplified to

$$\mathbf{U}^2 = \mathbf{I} + c^2((\mathbf{I} - \mathbf{S}^2)^{-1}\mathbf{M} + (1 - c^2)\mathbf{I})^{-1}. \tag{62}$$

The U-tensor represents the effect of interaction between the reinforcing inclusions and the matrix cracks. This becomes clear when eqn (58) is compared to eqn (56).

It is interesting to note that a similar simple measure for the interaction effect between reinforcing inclusions and cracks cannot be derived from the expression for the stiffness $\mathbf{L}^C$.

5. INTERPRETATION AND DISCUSSION OF RESULTS

In order to investigate the strengthening effect of the reinforcing inclusions, the energy release rate is determined for a representative matrix crack in the composite material.

The matrix of the composite material is assumed to be brittle and phase 1 is interpreted as a representative matrix crack. $\mathbf{M}^C$ is assumed to be determined according to eqn (58).

Assuming that the stresses are prescribed on the boundary according to eqn (1), Hill[21] showed that the total strain energy, W, in the representative volume element is given by

$$W = \frac{V}{2}\boldsymbol{\sigma}^*\mathbf{M}^C\boldsymbol{\sigma}^*. \tag{63}$$

The work done by the external forces can be written as

$$\int_{\delta(V)} \mathbf{u}\cdot\boldsymbol{\sigma}\cdot\mathbf{n}\,\mathrm{d}A = \int_{\delta(V)} \mathbf{u}\cdot\boldsymbol{\sigma}^*\cdot\mathbf{n}\,\mathrm{d}A$$
$$= \int_V \boldsymbol{\varepsilon}\boldsymbol{\sigma}^*\,\mathrm{d}V = V\{\boldsymbol{\varepsilon}\}^V\boldsymbol{\sigma}^* = V\boldsymbol{\sigma}^*\mathbf{M}^C\boldsymbol{\sigma}^*. \tag{64}$$

Thus the potential energy, W^P, defined by

$$W^P = W - \int_{\delta(V)} \mathbf{u}\cdot\boldsymbol{\sigma}\cdot\mathbf{n}\,\mathrm{d}A \tag{65}$$

can be written as

$$W^P = -\frac{V}{2}\boldsymbol{\sigma}^*\mathbf{M}^C\boldsymbol{\sigma}^*. \tag{66}$$

A simple Griffith criterion for the growth of the penny-shaped crack in question can now be set up, the formula relating the surface energy required for crack growth and the corresponding energy release rate:

$$\gamma\frac{\mathrm{d}(2\pi(a)^2)}{\mathrm{d}a} \leqq -\frac{\partial W^P}{\partial a}. \tag{67}$$

Here γ represents the specific surface energy or rather the specific work of fracture related to the crack surface.

Introducing the expression for W^P, eqn (66), we can introduce a macroscopically homogeneous critical stress by

$$\gamma\frac{\mathrm{d}(2\pi(a)^2)}{\mathrm{d}a} = \frac{V}{2}\boldsymbol{\sigma}^{cr}\frac{\partial\mathbf{M}^C}{\partial a}\boldsymbol{\sigma}^{cr}. \tag{68}$$

When the displacements are prescribed as in eqn (2), the potential energy is given by

$$W^P = \frac{V}{2}\boldsymbol{\varepsilon}^*\mathbf{L}^C\boldsymbol{\varepsilon}^* \tag{69}$$

thus an equivalent macroscopically homogeneous critical strain can be defined by

$$\gamma\frac{\partial(2\pi(a)^2)}{\partial a} = -\frac{V}{2}\boldsymbol{\varepsilon}^{cr}\frac{\partial\mathbf{L}^C}{\partial a}\boldsymbol{\varepsilon}^{cr}. \tag{70}$$

Since $\mathbf{L}^C = (\mathbf{M}^C)^{-1}$ it is easily shown that eqns (68) and (70) are totally equivalent under the assumption that

$$\boldsymbol{\sigma}^{cr} = \mathbf{L}^C\boldsymbol{\varepsilon}^{cr}. \tag{71}$$

The case of one penny-shaped crack in an otherwise homogeneous representative volume element is described by eqn (56) or (55), and the critical stress can be determined by

$$\frac{a}{2\gamma}\,\boldsymbol{\sigma}^{cr}\mathbf{F}^1\mathbf{M}^0\boldsymbol{\sigma}^{cr} = 1 \tag{72}$$

according to eqn (68). The component form of eqn (72) can be found in Ref. [5], where it is also mentioned that eqn (72) corresponds to the classical solution for a penny-shaped crack in an infinite medium, see e.g. Ref. [26].

The critical stress for the same penny-shaped matrix crack in a composite material can be written as

$$\frac{a}{2\gamma}\,\boldsymbol{\sigma}^{cr}\mathbf{U}^2\mathbf{F}^1\mathbf{M}^0\boldsymbol{\sigma}^{cr} = 1 \tag{73}$$

according to eqns (68) and (58).

The corresponding critical strain is determined from

$$\boldsymbol{\varepsilon}^{cr} = \mathbf{M}^C\boldsymbol{\sigma}^{cr} \tag{74}$$

rather than from eqn (70) which is a fairly complicated expression.

It is interesting to note that when the stiffness of phase 2 is negligible, which means that we are considering a penny-shaped crack in a porous material, then $\mathbf{U}^2$ can be written as

$$\begin{aligned}\mathbf{U}^2 &= \mathbf{I}+c^2(((\{(\mathbf{I}-\mathbf{S}^2)^{-1}(\mathbf{I}-\mathbf{S}^2)\}^{\omega})^{-1}-c^2\mathbf{I})^{-1}\\ &= \mathbf{I}+c^2(\mathbf{I}-c^2\mathbf{I})^{-1} = \mathbf{I}\frac{1}{1-c^2}.\end{aligned} \tag{75}$$

Writing G for the energy release rate for a penny-shaped crack in a porous medium and G^0 for the energy release rate for the same penny-shaped crack in the same medium but with no porosity, then we find from eqns (72) and (73) that

$$\frac{G}{G^0} = \frac{1}{1-c^2} \tag{76}$$

when a macroscopically homogeneous stress is prescribed.

Equation (76) *is independent of the shape and orientation of the porosity*. Note also that *the result is valid for both the crack opening stress states*: normal and shear stress relative to the crack plane (producing mode *I* and mixed shear cracking). Thus eqn (76) represents a generalization of the result presented in Ref. [18], which only covered the case of an aligned crack like porosity.

When phase 2 does not represent a porosity, then eqn (73) cannot be interpreted as easily as the above mentioned. Assuming that the reinforcing inclusions are axially symmetrical and aligned with an axis perpendicular to the penny-shaped crack surface, then the U-tensor is transversely isotropic with the same axis of symmetry as $\mathbf{F}^1$, which means that the decomposition technique already mentioned in Section 4 can be used to evaluate and decompose the fourth order product in eqn (73) using expression (62) for $\mathbf{U}^2$. If, alternatively, the reinforcing inclusions are axially symmetrical but randomized in space then the U-tensor is isotropic and determined by eqn (61), and again the fourth order tensor product in eqn (73) is transversely isotropic.

In order to calculate the average of a transversely isotropic fourth order tensor randomly distributed in space (this is necessary according to eqn (61)) it can be shown (see Ref. [24]) that if $\mathbf{A}$ is transversely isotropic with

$$\mathbf{A} = (a^1, a^2, a^3, a^4, a^5, a^6) \tag{77}$$

then

$$\{\mathbf{A}^{\text{random}}\}^{\omega} = (a^{\omega 1}, a^{\omega 2}) \tag{78}$$

with

$$a^{\omega 1} = \tfrac{1}{3}(2a^1 + a^2 + 2a^5 + 2a^6) \tag{79}$$

and

$$a^{\omega 2} = \tfrac{1}{5}(\tfrac{1}{3}a^1 + \tfrac{2}{3}a^2 + 2a^3 + 2a^4 - \tfrac{2}{3}a^5 - \tfrac{2}{3}a^6). \tag{80}$$

The decomposition, eqn (78), for the isotropic tensor is given by Hill[25].

In order to be able to calculate the product of the isotropic U-tensor and the transversely isotropic F-tensor by means of the formulas given in Ref. [23], we need the transversely isotropic decomposition of an isotropic fourth order tensor. This decomposition can be made with the following formula. Assuming that $\mathbf{A}$ is isotropic with

$$\mathbf{A} = (a^1, a^2) \tag{81}$$

then $\mathbf{A}$ can also be written as (see Ref. [24])

$$\mathbf{A} = (\tfrac{2}{3}a^1 + \tfrac{1}{3}a^2, \tfrac{1}{3}a^1 + \tfrac{2}{3}a^2, a^2, a^2, \tfrac{1}{3}(a^1 - a^2), \tfrac{1}{3}(a^1 - a^2)) \tag{82}$$

with any direction of the symmetry axis.

It is now possible to show that when the Cartesian coordinate system is orientated, so that the x_3-axis is normal to the crack surface, then eqn (73) can be rewritten as

$$\frac{2a(1-(\nu^0)^2)}{\gamma\pi E^0} u^2(\sigma_{33}^{\text{cr}})^2 + \frac{4a(1-(\nu^0)^2)}{\gamma\pi E^0(2-\nu^0)} u^4((\sigma_{13}^{\text{cr}})^2 + (\sigma_{23}^{\text{cr}})^2) + \frac{2a(1-(\nu^0)^2)}{\gamma\pi E^0} u^6(\sigma_{11}^{\text{cr}}\sigma_{33}^{\text{cr}} + \sigma_{22}^{\text{cr}}\sigma_{33}^{\text{cr}}) = 1 \tag{83}$$

where E^0 is Young's modulus for the matrix and where

$$\mathbf{U}^2 = (u^1, u^2, u^3, u^4, u^5, u^6) \tag{84}$$

with symmetry axis parallel to the x_3-axis.

Note that when $c^2 = 0$, i.e. when no reinforcing inclusions are present, then

$$\mathbf{U}^2 = \mathbf{I} = (1, 1, 1, 1, 0, 0) \tag{85}$$

and now the first and the second term in eqn (83) represent the dimensionless energy release rate for normal and shear stress applied to a penny-shaped crack in an (infinite) homogeneous medium producing mode I and mixed shear mode, respectively. Thus u^2 and u^4 represent the changes in the energy release rate for normal and shear stress respectively due to the reinforcing inclusions. (The terms "normal" and "shear" referring to the crack surface.) Note that when $u^6 \neq 0$, then σ_{11} and σ_{22} can also contribute to the energy release rate when $\sigma_{33} \neq 0$.

The factors u^2, u^4 and u^6 have been plotted in Figs 1–10 as functions of the volume concentration of the reinforcing inclusions, c^2. Also, the effect of stiffness, geometry and orientation is shown: the factors u^2 and u^4 are shown for $E^2/E^0 = 50$ and 10, different aspect ratios (l^2) of the inclusions are considered ($l^2 \to 0$ (platelets), $l^2 = 1$ (spheres), $l^2 = 10$, $l^2 = 20$ and $l^2 \to \infty$), and finally aligned as well as randomized inclusions are considered.

It is interesting to note that the platelets are not causing any reduction in the energy

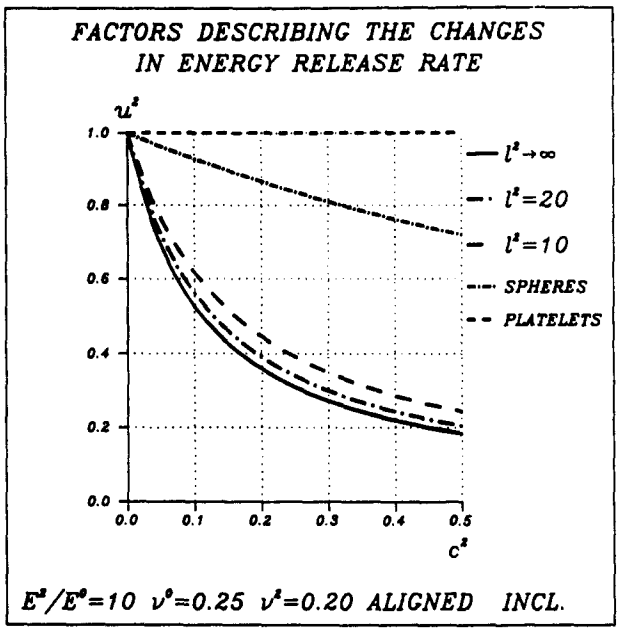

Fig. 1. The factor describing changes in G for a penny-shaped crack loaded with normal stress. The reinforcing inclusions are assumed to be aligned with an axis perpendicular to the crack surface.

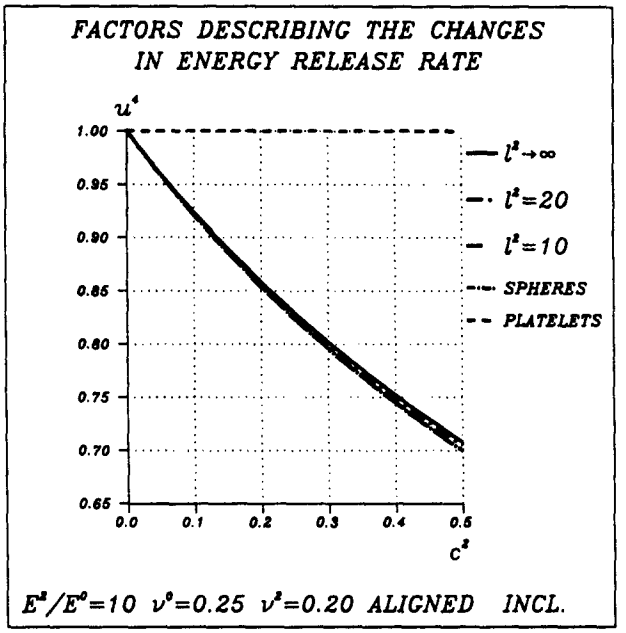

Fig. 2. The factor describing changes in G for a penny-shaped crack loaded with shear stress. The reinforcing inclusions are assumed to be aligned with an axis perpendicular to the crack surface.

release rates when they are aligned with the penny-shaped crack (though they are causing stiffness changes). But when the inclusions are randomized, then the platelets are causing the *largest* reductions in the energy release rates among the geometries considered here.

Note also, that the factor u^2 depends very much on the shape of the inclusions in the aligned case, while u^4 is almost independent of the inclusions shape in the range $1 \leqq l^2 < \infty$. However, when the inclusions are randomized, then u^2 and u^4 depend on l^2 in almost the same way. In the range $1 \leqq l^2 < \infty$ the infinitely long fibres are reducing the energy release rate the most, except in the case of aligned inclusions, factor u^4 and the energy release rate is always reduced with an increasing volume fraction of reinforcing inclusions.

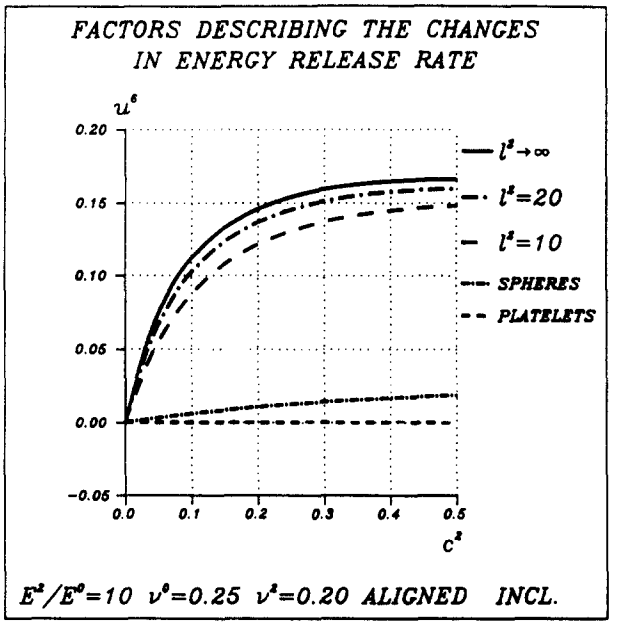

Fig. 3. The factor describing the additional energy release rate for a penny-shaped crack due to lateral tension. The reinforcing inclusions are assumed to be aligned with an axis perpendicular to the crack surface.

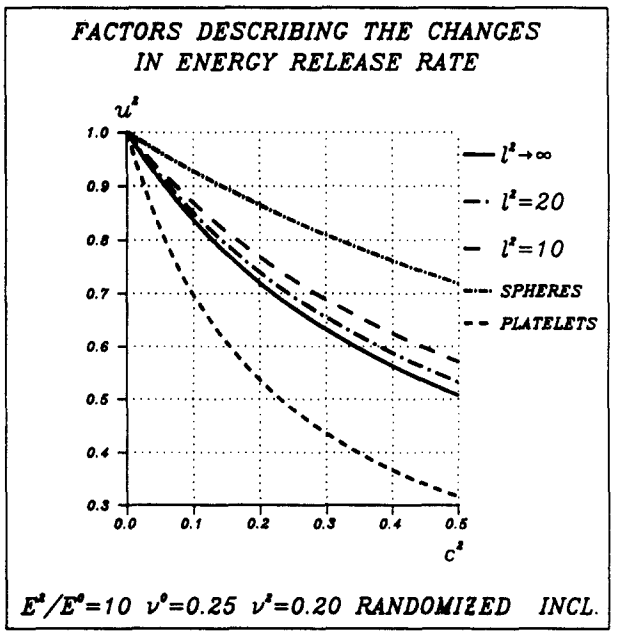

Fig. 4. The factor describing changes in G for a penny-shaped crack loaded with normal stress. The reinforcing inclusions are assumed to be randomly distributed in the surrounding matrix.

With regard to the stiffness effect it is interesting to compare Figs 1, 2, 7 and 8. While an increasing stiffness ratio, E^2/E^0 greatly reduces the u^2-factor (especially in the range $10 \leqq l^2 < \infty$), the u^4-factor is practically unchanged. In the randomized case both u^2 and u^4 is reduced when the stiffness ratio is increased (compare Figs 4, 5, 9 and 10), however, the effect still depends on the geometry of the inclusions.

When comparing the u^2-factor in Fig. 1 with the results for G/G^0 given by Taya[18] Fig. 7, it seems that Taya's results have been re-established in this special case.

The factor u^6 is significant in the case of aligned inclusions (see Figs 3 and 6) and very dependent on the shape of the inclusions. The positive value of u^6 corresponds to the fact that

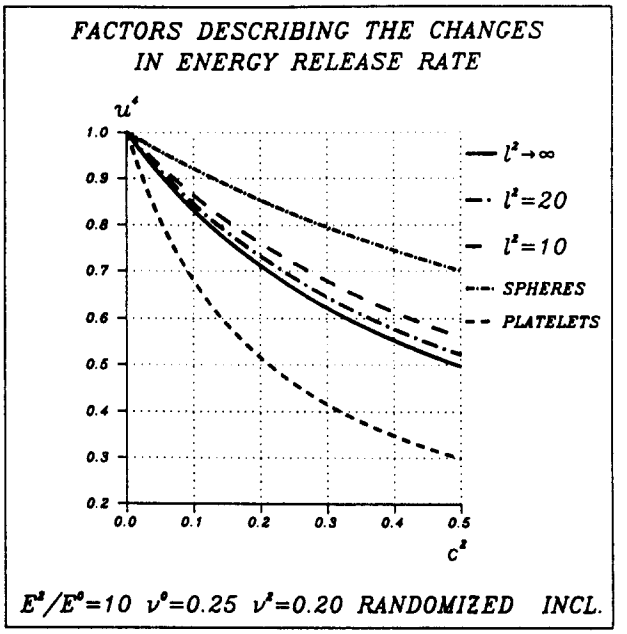

Fig. 5. The factor describing changes in G for a penny-shaped crack loaded with shear stress. The reinforcing inclusions are assumed to be randomly distributed in the surrounding matrix.

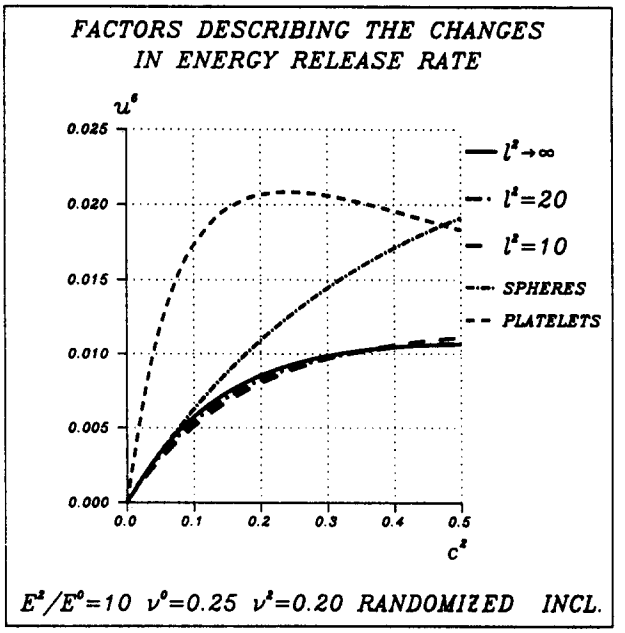

Fig. 6. The factor describing the additional energy release rate for a penny-shaped crack due to lateral tension. The reinforcing inclusions are assumed to be randomly distributed in the surrounding matrix.

a lateral tension applied to a unidirectional fibre reinforced composite material with fibres considerably stiffer than the matrix produces longitudinal *compression* in the fibre for most combinations of Poisson's ratio in the matrix and in the fibre. This means that a longitudinal tension field is produced in the matrix around the fibres. Thus, if matrix cracks with a surface perpendicular to the fibres are present in the matrix, then a lateral tension field can produce a crack opening stress field in the matrix. The fact that a lateral tension usually produces longitudinal compression in a fibre embedded in a matrix follow from the Eshelby solution[16] for one infinitely long fibre embedded in a matrix with a homogeneous stress

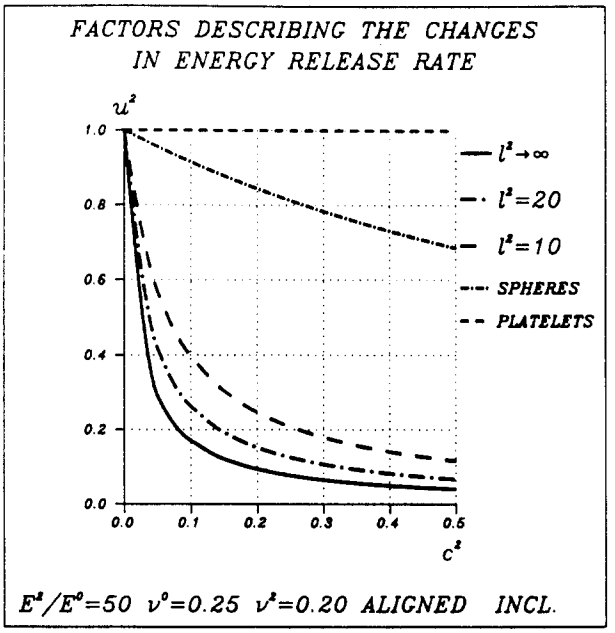

Fig. 7. The factor describing changes in G for a penny-shaped crack loaded with normal stress. The reinforcing inclusions are assumed to be aligned with an axis perpendicular to the crack surface.

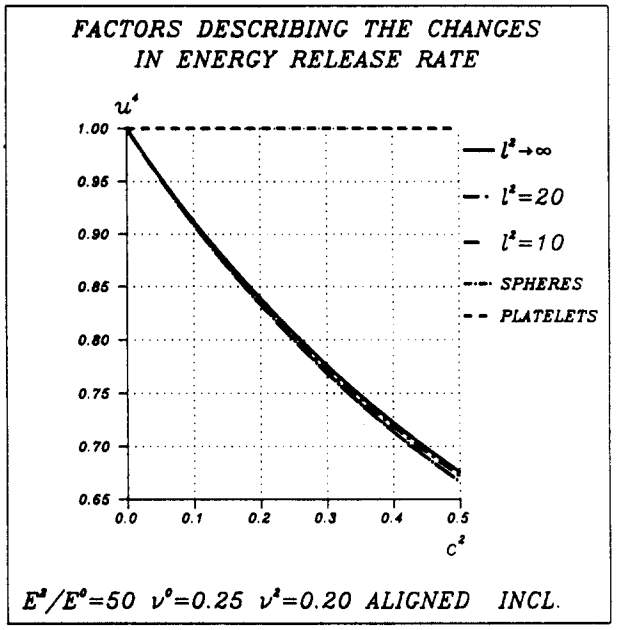

Fig. 8. The factor describing changes in G for a penny-shaped crack loaded with shear stress. The reinforcing inclusions are assumed to be aligned with an axis perpendicular to the crack surface.

field σ^0 far from the inclusion. The stress field σ^2 in the fibre is given by

$$\sigma^2 = (\mathbf{Q}^2(\mathbf{M}^2 - \mathbf{M}^0) + \mathbf{I})^{-1}\sigma^0 \tag{86}$$

or

$$\sigma^2 = (\mathbf{S}^2(\mathbf{M}^0 - \mathbf{M}^2) + \mathbf{M}^2)^{-1}\mathbf{M}^0\sigma^0 \tag{87}$$

where $\mathbf{S}^2$ and $\mathbf{Q}^2$ correspond to an infinitely long inclusion. If a lateral plane hydrostatic stress field with intensity σ_p^0 is present in the matrix far from the inclusion, then it can be

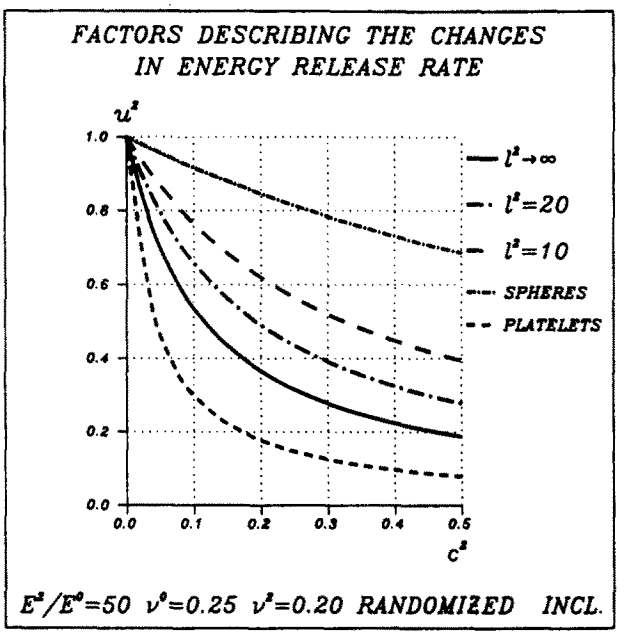

Fig. 9. The factor describing changes in G for a penny-shaped crack loaded with normal stress. The reinforcing inclusions are assumed to be randomly distributed in the surrounding matrix.

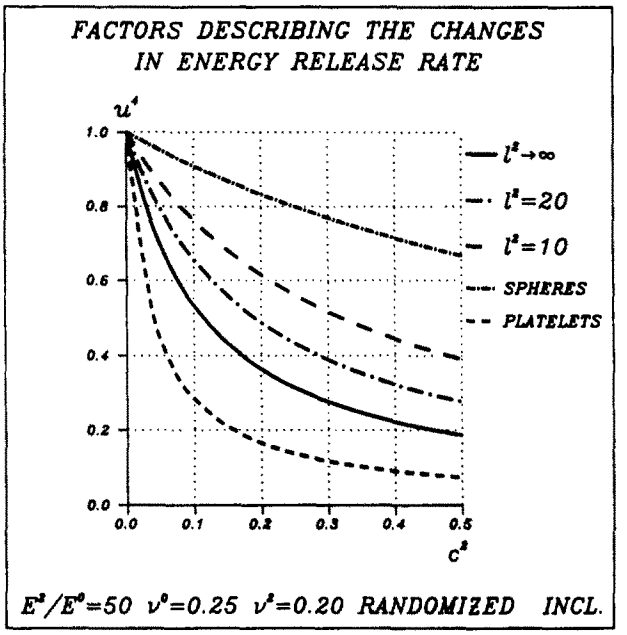

Fig. 10. The factor describing changes in G for a penny-shaped crack loaded with shear stress. The reinforcing inclusions are assumed to be randomly distributed in the surrounding matrix.

shown from eqn (87) (see Ref. [24]) that the ratio between the longitudinal stress in the fibre and the intensity of the plane hydrostatic stress field in the matrix is given by

$$\frac{\sigma_{33}^2}{\sigma_p^0} = -\frac{E[(1+\nu^0)\nu^0 E+(1-\nu^2)\nu^0-2\nu^2]}{2[E(1+\nu^0)+(1+\nu^2)(1-2\nu^2)]} \tag{88}$$

with

$$E = \frac{E^2}{E^0}. \tag{89}$$

From this expression it is clear that in the case investigated in Fig. 3 with $E = 10$, $\nu^0 = 0.25$ and $\nu^2 = 0.20$ expression (88) gives a negative value of σ_{33}^2/σ_p^0.

If, however, $E = 10$, $\nu^0 = 0$, and $\nu^2 = 0.20$, then σ_{33}^2/σ_p^0 is positive, i.e. a lateral plane tension field in the matrix produces longitudinal tension in the fibres according to eqn (88), and thus a longitudinal compression field arises in the matrix around the fibre. Calculating u^6 in the case of aligned long inclusions with $E = 10$, $\nu^0 = 0$, and $\nu^2 = 0.20$, u^6 becomes negative, i.e. a lateral tension field reduces the energy release rate related to σ_{33} because of its crack closing effect.

6. CONCLUSION

A composite material theory developed by Levin[15] taking account of the interaction between the inclusions has been generalized so that it can describe composite materials with more than one type of inclusions. This model has been used to evaluate the energy release rate for a penny-shaped crack in a composite material. Having interpreted the results, the following conclusions can be made:

(1) With a prescribed stress-field the changes in energy release rate for a penny-shaped crack due to the reinforcing inclusions can be described by a single fourth order tensor, U.

(2) In the case where the reinforcing inclusions are pores a very simple result is obtained for the influence of the porosity on the energy release rate. The result contains Taya's[18] as a special case.

(3) When interpreting the physical significance of the U-tensor the decomposition technique described by Walpole[23] is very convenient.

(4) When the reinforcing inclusions are aligned the infinitely long fibres are the most efficient in reducing the energy release rate. However, when randomized inclusions are considered, then the flat disc shaped inclusions, "platelets", are the most efficient. In any case, the efficiency of the inclusions is increased when the volume fraction is increased.

(5) It seems that the results obtained for long aligned inclusions (fibres) correspond to Taya's[18].

(6) Finally, it is shown that a lateral tension in an aligned fibre composite material can contribute to the energy release rate of matrix cracks perpendicular to the fibres when a longitudinal stress component is also present.

REFERENCES

1. C. K. H. Dharan, Fracture mechanics of composite materials. *J. Engng Mat. Tech.* **100**, 233–347 (1978).
2. Y. Korczynskyj, S. J. Harris and J. G. Morley, The influence of reinforcing fibres on the growth of cracks in brittle matrix composites. *J. Mater. Sci.* **16**, 1533–1547 (1981).
3. A. P. S. Selvadurai, Concentrated body force loading of an elastically bridged penny shaped flaw in a unidirectional fibre reinforced composite. *Int. J. Fracture* **21**, 149–159 (1983).
4. T. Mori and T. Mura, An inclusion model for crack arrest in fiber reinforced materials. *Mech. Mater.* **3**, 193–198 (1984).
5. H. Stang, A double inclusion model for microcrack arrest in fibre reinforced brittle materials. Submitted to *J. Mech. Phys. Solids* (1986).
6. J. R. Bristow, Microcracks and the static and dynamic elastic constants of annealed and heavily cold-worked metals. *Br. J. Appl. Phys.* **11**, 81 (1960).
7. J. B. Walsh, New analysis of attenuation in partially melted rock. *J. Geophys. Res.* **74**(17), 4333–4337 (1969).
8. R. L. Salganik, Mechanics of bodies with many cracks. *Izv. AN SSSR, Mekh. Tverd. Tela* **8**(4), 149–158 (1973) (*Mech. Solids* 135–143).
9. B. Budiansky and R. J. O'Connell, Elastic moduli of a cracked solid. *Int. J. Solids Structures* **12**, 81–97 (1976).
10. B. Budiansky, On the elastic moduli of some heterogeneous materials. *J. Mech. Phys. Solids* **13**, 223–227 (1965).
11. R. Hill, A self-consistent mechanics of composite materials. *J. Mech. Phys. Solids* **13**, 213–222 (1965).
12. A. Hoenig, Elastic moduli of a non-randomly cracked body. *Int. J. Solids Structures* **15**, 137–154 (1979).
13. J. R. Willis, Bounds and self-consistent estimates for the overall properties of anisotropic composites. *J. Mech. Phys. Solids* **25**, 185–202 (1977).
14. H. Horii and S. Nemat-Nasser, Overall moduli of solids with microcracks: load-induced anisotropy. *J. Mech. Phys. Solids* **31**, 155–171 (1983).
15. V. M. Levin, Determination of effective elastic moduli of composite materials. *Dokl. Akad. Nauk SSSR* **220**(5), 1042–1045 (1975) (*Sov. Phys. Dokl.* **20**(2), 147–148 (1975)).
16. J. D. Eshelby, The determination of the elastic field of an ellipsoidal inclusion and related problems. *Proc. R. Soc. London* **A241**, 376–396 (1957).

17. N. Laws, G. J. Dvorak and M. Hejazi, Stiffness changes in unidirectional composites caused by crack systems. *Mech. Mater.* **2**, 123–137 (1983).
18. M. Taya, On stiffness and strength of an aligned short-fiber reinforced composite containing penny-shaped cracks in the matrix. *J. Composite Mater.* **15**, 198–210 (1981).
19. M. Taya and T.-W. Chou, On two kinds of ellipsoidal inhomogeneities in an infinite elastic body: an application to a hybrid composite. *Int. J. Solids Structures* **17**, 553–563 (1981).
20. T. Mori and K. Tanaka, Average stress in matrix and average elastic energy of materials with misfitting inclusions. *Acta Metal.* **21**, 571–574 (1973).
21. R. Hill, Elastic properties of reinforced solids: some theoretical principles. *J. Mech. Phys. Solids* **11**, 357–372 (1963).
22. V. M. Levin, On the stress concentration in inclusions in composite materials. *PMM* **41**(4), 735–743 (1977) (*J. Appl. Math. Mech.* 753–761).
23. L. J. Walpole, Elastic behavior of composite materials: theoretical foundations. *Adv. Appl. Mech.* **21**, 169–242 (1981).
24. H. Stang, A composite material theory and its application to the description of cement composites loaded in tension. Ph.D. thesis, Department of Structural Engineering, Technical University of Denmark, Series R, No. 193 (1984), in Danish.
25. R. Hill, Continuum micro-mechanics of elastoplastic polycrystals. *J. Mech. Phys. Solids* **13**, 89–101 (1965).
26. G. C. Sih and H. Liebowitz, Mathematical theories of brittle fracture. In *Fracture, an Advanced Treatise* (Edited by H. Liebowitz), Vol. 2, Chap. 2. Academic Press, New York (1968).